Dark Quarkonium Formation in the Early Universe

University of Toronto, Toronto, CAN

Gabriel Lee

Cornell University/Korea University
1802.xxxxx with M. Geller, S. Iwamoto, Y. Shadmi, O. Telem

Feb 15, 2018

A Social Media Profile of Dark Matter

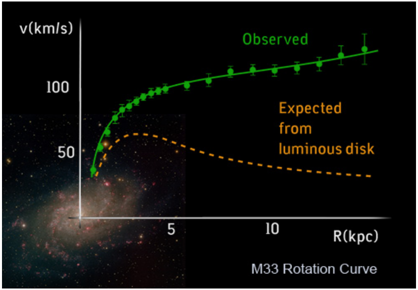

A Social Media Profile of Dark Matter

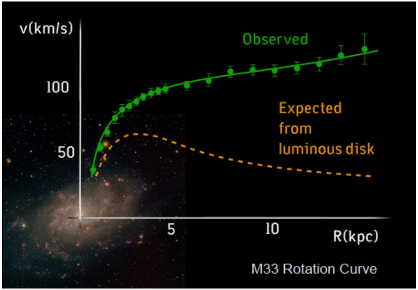

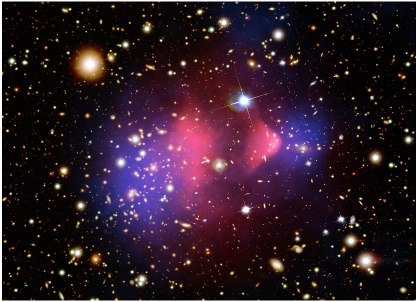

A Social Media Profile of Dark Matter

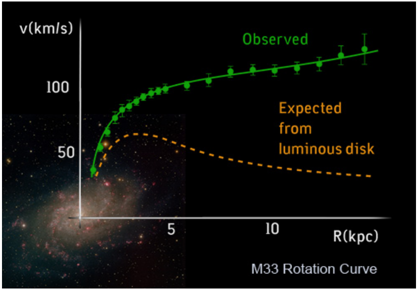

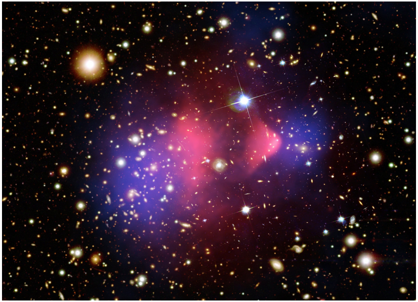

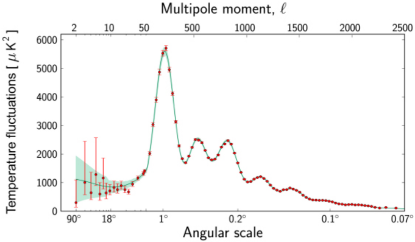

A Social Media Profile of Dark Matter

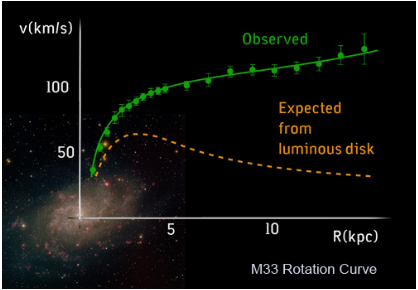

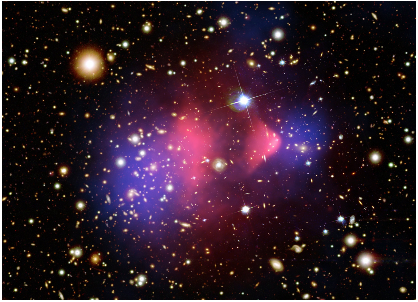

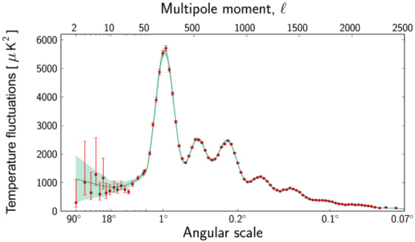

Gravitational evidence

- galactic
- cluster
- cosmological

Catch Me If You Can

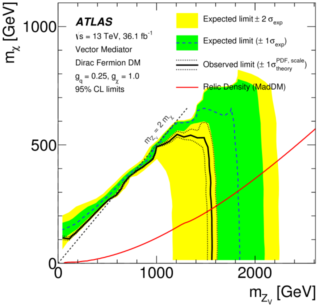

ATLAS 1711.03301

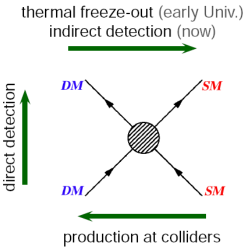

Catch Me If You Can

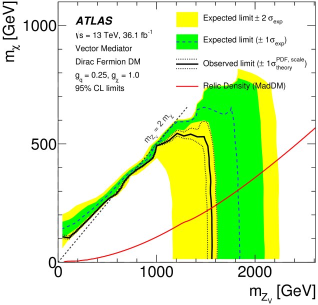

ATLAS 1711.03301

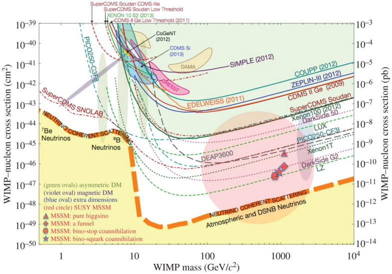

Cooley 1410.4960; Billard, Figueroa-Feliciano, Strigari 1307.5458

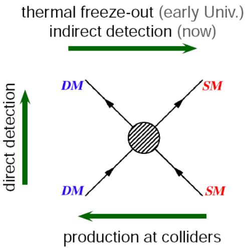

Catch Me If You Can

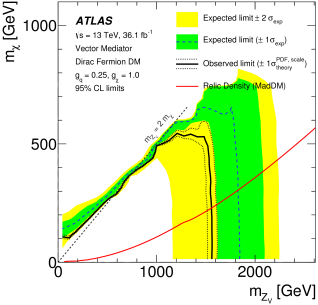

ATLAS 1711.03301

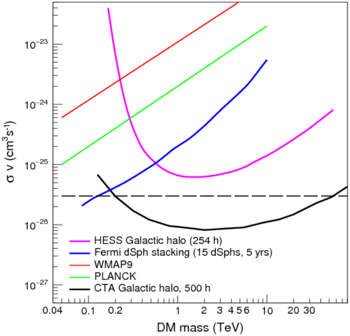

Morselli et al. 1709.01483

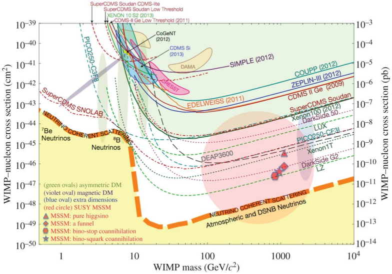

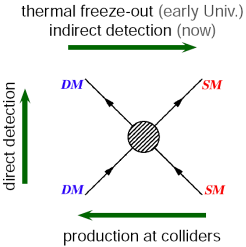

Cooley 1410.4960; Billard, Figueroa-Feliciano, Strigari 1307.5458

WIMP Miracle

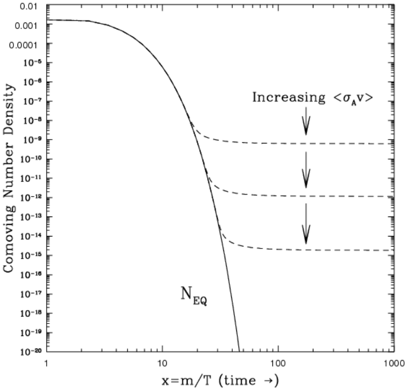

If DM was in thermal contact with the SM in the early universe, the observed DM relic density parameter is

$$0.11 \sim \Omega h^2 = \frac{3 \times 10^{-27}\ \mathrm{cm}^3/\mathrm{s}}{\langle \sigma_{\mathrm{ann}} v_{\mathrm{rel}} \rangle}$$

$$\sim 2.5 \times 10^{-10}\ \mathrm{GeV}^{-2} \frac{m^2}{\alpha^2}\ ,$$

if s-wave scattering dominates annihilation cross section.

WIMP Miracle

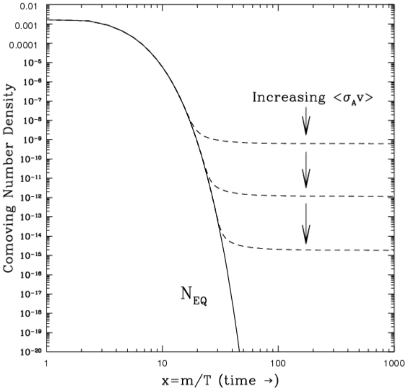

If DM was in thermal contact with the SM in the early universe, the observed DM relic density parameter is

$$0.11 \sim \Omega h^2 = \frac{3 \times 10^{-27}\,\mathrm{cm}^3/\mathrm{s}}{\langle \sigma_{\mathrm{ann}} v_{\mathrm{rel}} \rangle}$$
$$\sim 2.5 \times 10^{-10}\,\mathrm{GeV}^{-2}\,\frac{m^2}{\alpha^2}\,,$$

if s-wave scattering dominates annihilation cross section.

For weak-scale masses and couplings $m \sim 10^3$ GeV, $\alpha \sim 0.6^2/(4\pi) \sim 0.03$,

$$2.5 \times 10^{-10}\,\frac{10^6}{10^{-3}} \sim 0.25\,.$$

DM Mass Parameter Space

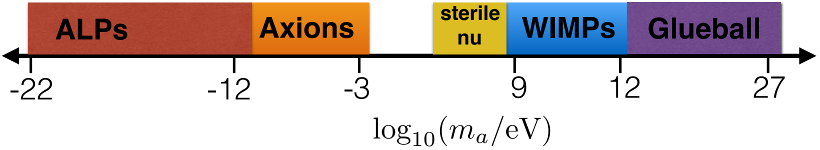

from B. Safdi

DM Mass Parameter Space

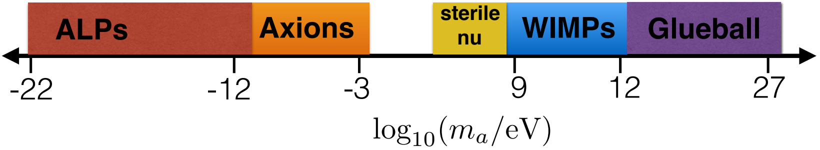

from B. Safdi

- Hidden photons
- Ultra-light scalar fields
- Axions
- Q-balls

- Neutralinos
- Gravitinos
- Sterile neutrinos
- Dark hadrons

DM Mass Parameter Space

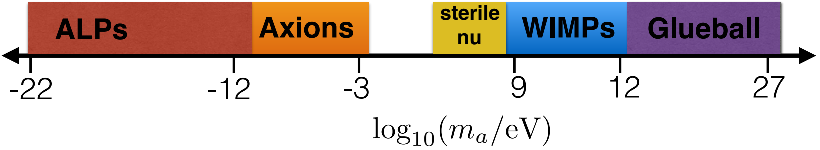

from B. Safdi

- Hidden photons
- Ultra-light scalar fields
- Axions
- Q-balls
- Neutralinos
- Gravitinos
- Sterile neutrinos
- Dark hadrons

No shortage of either bosonic or fermionic candidates.

Tim Tait's DM Venn Diagram

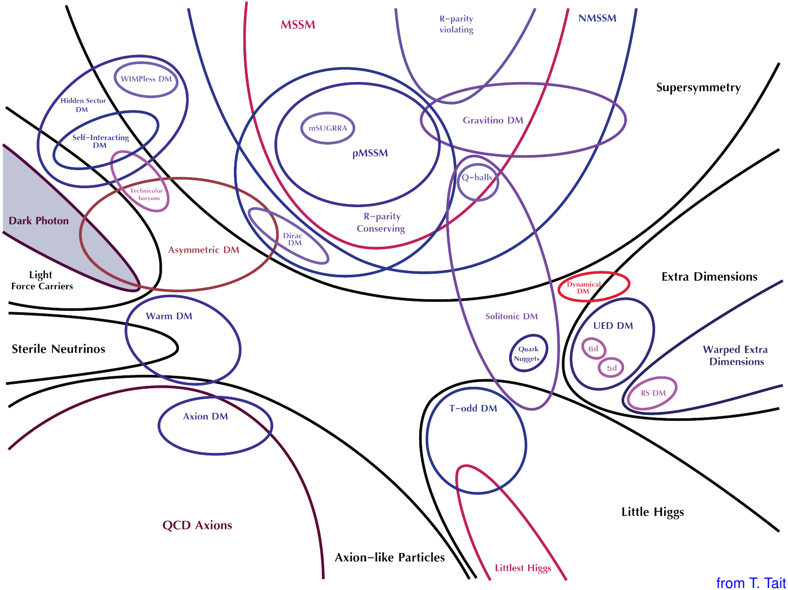

from T. Tait (c. 2009)

Beyond One-Particle Dark Sectors

Motivations:

- asymmetric DM (connecting DM to baryon asymmetry),
- excited or inelastic DM (novel methods for direct detection),
- different cosmology (more possibilities for obtaining present relic density).

Beyond One-Particle Dark Sectors

Motivations:

- asymmetric DM (connecting DM to baryon asymmetry),
- excited or inelastic DM (novel methods for direct detection),
- different cosmology (more possibilities for obtaining present relic density).

Confining dynamics give us nontrivial spectra!

Beyond One-Particle Dark Sectors

Motivations:

- asymmetric DM (connecting DM to baryon asymmetry),
- excited or inelastic DM (novel methods for direct detection),
- different cosmology (more possibilities for obtaining present relic density).

Confining dynamics give us nontrivial spectra!

- Generic in dark matter models with nonabelian hidden sectors.
- Below some confinement scale, “coloured” particles must combine to form singlets.
- The hadrons can now have qualitatively different interactions than the constituents (at the very least, nonperturbative).
- Generic in most BSM model building: strings, SUSY, strong dynamics, etc.

"Colour"-Singlet States in Nonabelian Dark Matter

- Glueballs (pure Yang-Mills) — Forestell, Morrissey, Sigurdson 1710.06447
- Quirks (heavy fundamentals) — Kribs, Roy, Terning, Zurek 0909.2034
- Mesons and baryons (light fundamentals) — Kang, Luty, Nasri 0611322; Appelquist et al. 1503.04203; Harigaya et al. 1606.00159
- R-hadrons (heavy adjoints) — e.g., gluinos in Arvanitaki et al. 0812.2075; Feng & Shadmi 1102.0282
- Heavy adjoint bound states — De Luca et al. 1801.01135
- Nuclear DM — e.g., Hardy et al. 1504.05419; Wise & Zhang 1407.4121 + An 1604.01776; Gresham, Hou, Zurek 1707.02313
- Sexaquarks — Farrar, 1708.08951
- Atomic DM — Kaplan et al. 0909.0753; Cyr-Racine & Sigurdson 1209.5752; Boddy et al. 1609.03592

Parameter space in (coupling, mass) varies widely!

Second-Stage Annihilation

Cosmology deviates from standard freeze-out scenario.

Second-Stage Annihilation

Cosmology deviates from standard freeze-out scenario.

- Below confinement scale, bound states have finite size dictated by the light coloured states ("brown muck").
- Hadrons can undergo a second stage of annihilation, reducing the relic density (and therefore allowing heavier dark matter masses).
- Argument: no symmetry dictates that the cross section should be smaller than the naïve geometric cross section.

Second-Stage Annihilation

Cosmology deviates from standard freeze-out scenario.

- Below confinement scale, bound states have finite size dictated by the light coloured states ("brown muck").
- Hadrons can undergo a second stage of annihilation, reducing the relic density (and therefore allowing heavier dark matter masses).
- Argument: no symmetry dictates that the cross section should be smaller than the naïve geometric cross section.

Which bound state formation (BSF) processes allow for a geometric cross section?

Unitarity Bound on DM Mass

Griest & Kamionkowski, Phys.Rev.Lett. 64, 615 (1990)

Upper limit on mass of DM once in thermal equilibrium with SM from partial-wave unitarity:

$$(\sigma_J) < \frac{4\pi(2J+1)}{m_X^2 v_{\rm rel}^2} \, .$$

Unitarity Bound on DM Mass

Griest & Kamionkowski, Phys.Rev.Lett. 64, 615 (1990)

Upper limit on mass of DM once in thermal equilibrium with SM from partial-wave unitarity:

$$(\sigma_J) < \frac{4\pi(2J+1)}{m_X^2 v_{\rm rel}^2}\,.$$

At freeze-out $m/T_f = 20$, $v_{\rm rel} \sim 2v \sim 2/\sqrt{10}$, and cross sections higher-order in J are suppressed by powers of $v_{\rm rel}^2/4 \sim 1/6$.

Unitarity Bound on DM Mass

Griest & Kamionkowski, Phys.Rev.Lett. 64, 615 (1990)

Upper limit on mass of DM once in thermal equilibrium with SM from partial-wave unitarity:

$$(\sigma_J) < \frac{4\pi(2J+1)}{m_X^2 v_{\rm rel}^2} \,.$$

At freeze-out $m/T_f = 20$, $v_{\rm rel} \sim 2v \sim 2/\sqrt{10}$, and cross sections higher-order in J are suppressed by powers of $v_{\rm rel}^2/4 \sim 1/6$.
Then using $J = 0$,

$$\Omega_X h^2 \sim 0.1 \gtrsim \frac{2.5 \times 10^{-10}\,\mathrm{GeV}^{-2}}{4\pi} m_X^2 v_{\rm rel}^2 \,,$$
$$\Rightarrow \left(\frac{m_X}{\mathrm{TeV}}\right)^2 \lesssim 10^4$$

Unitarity Bound on DM Mass

Griest & Kamionkowski, Phys.Rev.Lett. 64, 615 (1990)

Upper limit on mass of DM once in thermal equilibrium with SM from partial-wave unitarity:

$$(\sigma_J) < \frac{4\pi(2J+1)}{m_X^2 v_{\rm rel}^2}\,.$$

At freeze-out $m/T_f = 20$, $v_{\rm rel} \sim 2v \sim 2/\sqrt{10}$, and cross sections higher-order in J are suppressed by powers of $v_{\rm rel}^2/4 \sim 1/6$.
Then using $J = 0$,

$$\Omega_X h^2 \sim 0.1 \gtrsim \frac{2.5\times 10^{-10}\,\mathrm{GeV}^{-2}}{4\pi} m_X^2 v_{\rm rel}^2\,,$$
$$\Rightarrow \left(\frac{m_X}{\mathrm{TeV}}\right)^2 \lesssim 10^4$$

Can this bound be exceeded in the framework above?

Outline

Matter Content and Symmetries

Field	SU(N)	U(1)	Mass
$X, \bar{X}$	$N, \bar{N}$	$1, -1$	$m_X \gg \Lambda_D$
$q, \bar{q}$	$N, \bar{N}$	0	$m_q \sim \Lambda_D$

- Add a flavour symmetry to make X stable.
- The nonabelian gauge group is confining at a scale Λ_D.
- Below confinement temperature, $X, \bar{X}$ will form heavy-light mesons

$$H_X \equiv X\bar{q}\,, \quad \bar{H}_X \equiv \bar{X}q\,.$$

- Also possible to have an adjoint X without q: “R-hadron”-like colour-singlet states Xg.

Scales in Confined QCD

m_π, f_π, m_q

$\Big\updownarrow \; m_\pi^2 = \frac{V^3}{f_\pi^2}(m_u + m_d)$

$V \sim 230 \pm 30\,\mathrm{MeV}$

(QCD sum rules)

$T_c \sim 165\text{–}195\,\mathrm{MeV}$ (lattice)

$\Big\updownarrow \; \frac{T_c}{\sqrt{\sigma}} = 0.597(4) + \frac{0.45(3)}{N_c^2}$

$\sigma \sim 0.16\text{–}0.19\,\mathrm{GeV}^2$ $\xleftrightarrow{\sigma \sim \frac{C_F \Lambda_{\mathrm{QCD}}^2}{2\beta_0}}$ $\Lambda_{\mathrm{QCD}} \sim 332 \pm 17\,\mathrm{MeV}$

(Regge, pot'n model)

(4L $\overline{\mathrm{MS}}$ RG running)

Teper 0812.0085, Brambilla et al. 1010.5827, Simolo 0807.1501, RPP 2016

- In our toy model, Λ_D is determined by $\alpha_D(m_X), m_X$, both of which are free parameters.
- We will be concerned with the two ratios

$$\frac{T}{\Lambda_D} \lesssim \frac{T_c}{\Lambda_D} \lesssim 1\,,$$
$$\frac{m_X}{\Lambda_D} \gtrsim \mathcal{O}(10^2)\,.$$

Spectrum of Bound States

We can calculate the spectrum of X–$\bar{X}$ bound states using QM, modelling the interaction using a Cornell potential in analogy to quarkonium.

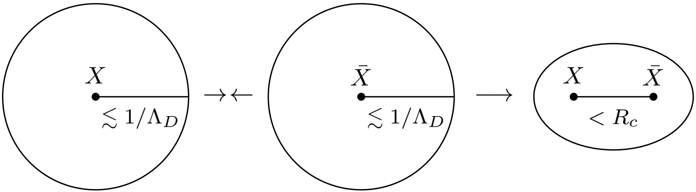

Spectrum of Bound States

We can calculate the spectrum of X–$\bar{X}$ bound states using QM, modelling the interaction using a Cornell potential in analogy to quarkonium.

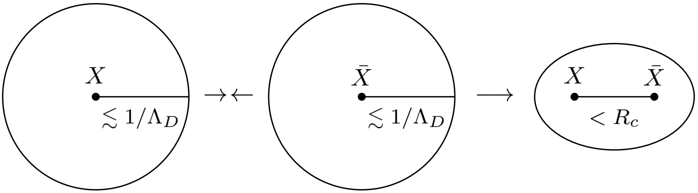

With light coloured states, the nonabelian force has finite range in the confined phase. To enforce this, we add a cutoff to the Cornell potential:

$$V(R) = \begin{cases} -\bar{\alpha}_D\left(\frac{1}{R} - \frac{1}{R_c}\right) + \Lambda_D^2(R - R_c) + V_0 & R < R_c\,, \\ V_0 & R > R_c\,. \end{cases}$$

Spectrum of Bound States

We can calculate the spectrum of X–$\bar{X}$ bound states using QM, modelling the interaction using a Cornell potential in analogy to quarkonium.

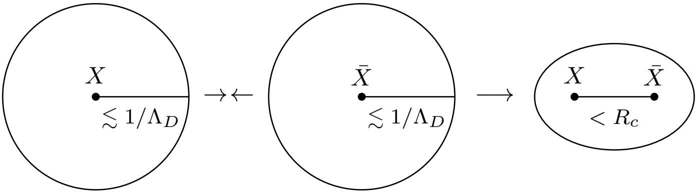

With light coloured states, the nonabelian force has finite range in the confined phase.
To enforce this, we add a cutoff to the Cornell potential:

$$V(R) = \begin{cases} -\bar{\alpha}_D \left(\frac{1}{R} - \frac{1}{R_c}\right) + \Lambda_D^2 (R - R_c) + V_0 & R < R_c\,, \\ V_0 & R > R_c\,. \end{cases}$$

How to determine R_c?

Heavy-Light Mesons

Consider D and B mesons in QCD.

Q	m_Q	m_{meson}
c	$1.3\,\text{GeV}$	$1865\,\text{MeV}$
b	$4.65\,\text{GeV (1S)}$	$5280\,\text{MeV}$

Heavy-Light Mesons

Consider D and B mesons in QCD.

Q	m_Q	m_{meson}
c	$1.3\,\text{GeV}$	$1865\,\text{MeV}$
b	$4.65\,\text{GeV}$ (1S)	$5280\,\text{MeV}$

In both cases, we have

$$m_{\text{meson}} - m_Q \sim 600\,\text{MeV}\,,$$

or about twice the "constituent mass" of a light quark.

Heavy-Light Mesons

Consider D and B mesons in QCD.

Q	m_Q	m_{meson}
c	$1.3\,\text{GeV}$	$1865\,\text{MeV}$
b	$4.65\,\text{GeV (1S)}$	$5280\,\text{MeV}$

In both cases, we have

$$m_{\text{meson}} - m_Q \sim 600\,\text{MeV}\,,$$

or about twice the "constituent mass" of a light quark.
Writing this parametrically as

$$m_{\text{meson}} - m_Q \sim \kappa_\Lambda \Lambda\,,$$

with $\Lambda \sim \sqrt{\sigma} \sim 400\,\text{MeV} \Rightarrow \kappa_\Lambda \sim 1.5$.

Bound States and the Potential Cutoff

A natural way to define the cutoff: the threshold for open production of two H_X hadrons. If this occurs in the linear regime of the potential, then

$$E_b^{\max} = \Lambda_D^2 r_c = 2\kappa_\Lambda \Lambda_D \,,$$

$$R_c = 2\frac{\kappa_\Lambda}{\Lambda_D} \sim \frac{3}{\Lambda_D} \,.$$

Bound States and the Potential Cutoff

A natural way to define the cutoff: the threshold for open production of two H_X hadrons.
If this occurs in the linear regime of the potential, then

$$E_b^{\max} = \Lambda_D^2 r_c = 2\kappa_\Lambda \Lambda_D \,,$$

$$R_c = 2\frac{\kappa_\Lambda}{\Lambda_D} \sim \frac{3}{\Lambda_D} \,.$$

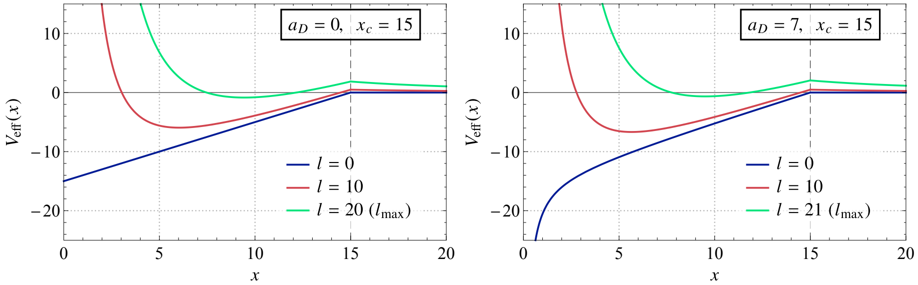

Spectrum Snapshot

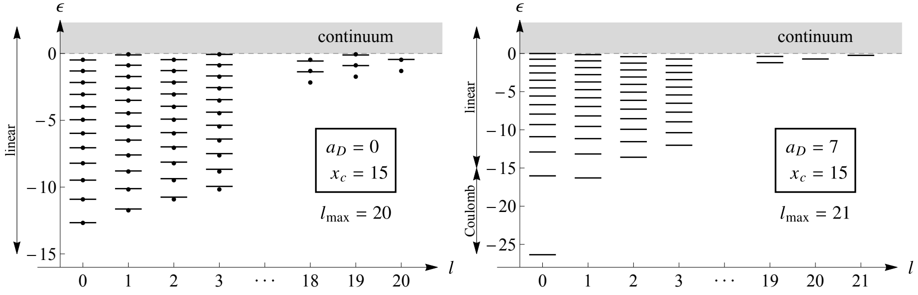

e.g., Quigg & Rosner, Phys.Rept. 56, 167 (1979); Hall & Saad 1411.2023

Spectrum Snapshot

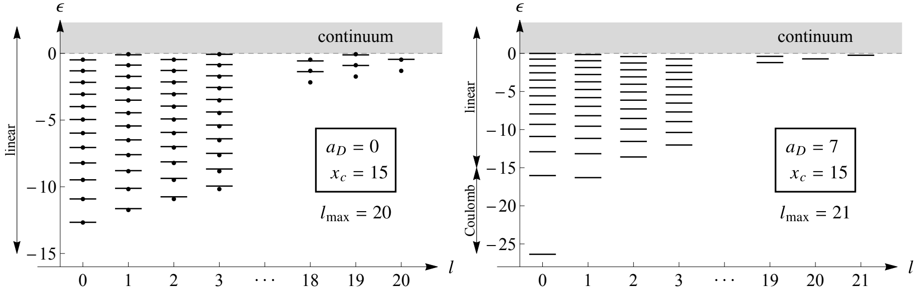

- hydrogenic: $E_{nl} \sim -\frac{\bar{\alpha}_D^2 \mu}{2n^2}$
- linear: $E_{nl} \propto \Lambda_D \left(\frac{\Lambda_D}{2\mu}\right)^{1/3} \left[\frac{3}{2}\pi\left(n + \frac{l}{2} - \frac{1}{4}\right)\right]^{2/3}$

e.g., Quigg & Rosner, Phys.Rept. 56, 167 (1979); Hall & Saad 1411.2023

Thermal History

—— m_X

X, g, q

—— $T_{f,X} \sim m_X/20$

g, q

—— $\Lambda_D \sim T_c$

hadrons

—— m_q

Thermal History

m_X

X, g, q

$T_{f,X} \sim m_X/20$

g, q

$\Lambda_D \sim T_c$

hadrons

m_q

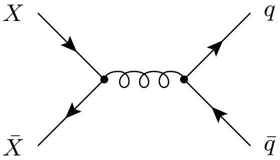

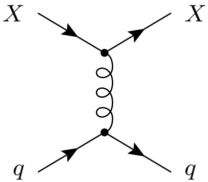

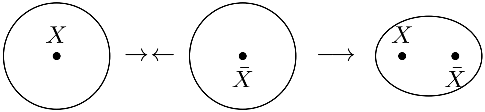

Outline

Setup

$$H_X + \bar{H}_X \to \left(X\bar{X}\right) + (q\bar{q})$$

Setup

$$H_X + \bar{H}_X \to \left(X\bar{X}\right) + (q\bar{q})$$

- Rigorous calculation for $m_q \lesssim \Lambda_D$ requires pNRQCD machinery (quarkonium).
- Regime with $m_q \gtrsim \Lambda_D$ can be treated using scattering theory in nonrelativistic QM.
- Here, calculation is analogous to H-$\bar{\mathrm{H}}$ rearrangement at low temperatures (e.g., for CPT tests)

$$\mathrm{H}(1s) + \bar{\mathrm{H}}(1s) \to \mathrm{Pn}(NLM) + \mathrm{Ps}(nlm)\,.$$

Kolos et al., PRA 11, 1792 (1975)

Froelich et al., PRL 84, 4577 (2000); Jonsell et al., PRA 64, 052712 (2001)

Jonsell et al., J. Phys. B: At. Mol. Opt. Phys. 37, 1195 (2004); Zygelman et al., PRA 69, 042715 (2004)

Setup

$$H_X + \bar{H}_X \to \left(X\bar{X}\right) + (q\bar{q})$$

- Rigorous calculation for $m_q \lesssim \Lambda_D$ requires pNRQCD machinery (quarkonium).
- Regime with $m_q \gtrsim \Lambda_D$ can be treated using scattering theory in nonrelativistic QM.
- Here, calculation is analogous to H-$\bar{\mathrm{H}}$ rearrangement at low temperatures (e.g., for CPT tests)

$$\mathrm{H}(1s) + \bar{\mathrm{H}}(1s) \to \mathrm{Pn}(NLM) + \mathrm{Ps}(nlm)\,.$$

Kolos et al., PRA 11, 1792 (1975)

Froelich et al., PRL 84, 4577 (2000); Jonsell et al., PRA 64, 052712 (2001)

Jonsell et al., J. Phys. B: At. Mol. Opt. Phys. 37, 1195 (2004); Zygelman et al., PRA 69, 042715 (2004)

From QM, the cross section in COM frame is

$$\frac{d\sigma}{d\Omega} = (2\pi)^2 \frac{k_f}{k_i} m_X m_q |\mathcal{M}|^2\,,$$

with matrix element

$$\mathcal{M} = 2\pi \left\langle \Psi_f\left(\mathbf{R}, \mathbf{r}_q, \mathbf{r}_{\bar{q}}\right)\right| \mathcal{H}_{\mathrm{tr}} \left|\Psi_i\left(\mathbf{R}, \mathbf{r}_q, \mathbf{r}_{\bar{q}}\right)\right\rangle\,.$$

Semiclassical Arguments

Kang, Luty, Nasri hep-ph/0611322

- For $m_q > \Lambda_D$, distance b/w X and $\bar{q}$ in H_X and the average force between them are

$$a_q \sim \frac{1}{\alpha_D m_q}\,,\ F \sim \frac{\bar{\alpha}_D}{a_q^2} \sim \alpha_D^3 m_q^2\,.$$

Semiclassical Arguments

Kang, Luty, Nasri hep-ph/0611322

- For $m_q > \Lambda_D$, distance b/w X and $\bar{q}$ in H_X and the average force between them are

$$a_q \sim \frac{1}{\alpha_D m_q}\,,\ F \sim \frac{\bar{\alpha}_D}{a_q^2} \sim \alpha_D^3 m_q^2\,.$$

- The velocity is set by the temperature, which is assumed to be of order the binding energy $v \sim \sqrt{T/m_X} \sim \bar{\alpha}_D \sqrt{m_q/m_X}$.
- When a free X with initial velocity v comes with a distance a_q of a $\bar{q}$, its velocity changes by

$$\frac{\Delta v}{v} \sim \frac{1}{v}\frac{F}{m_X}\Delta t \sim \frac{1}{v}\frac{F}{m_X}\frac{a_q}{v} \sim \frac{\alpha_D^2 m_q}{m_X v^2} \sim 1\,.$$

Semiclassical Arguments

Kang, Luty, Nasri hep-ph/0611322

- For $m_q > \Lambda_D$, distance b/w X and $\bar{q}$ in H_X and the average force between them are

$$a_q \sim \frac{1}{\alpha_D m_q}\,, \; F \sim \frac{\bar{\alpha}_D}{a_q^2} \sim \alpha_D^3 m_q^2\,.$$

- The velocity is set by the temperature, which is assumed to be of order the binding energy $v \sim \sqrt{T/m_X} \sim \bar{\alpha}_D \sqrt{m_q/m_X}$.
- When a free X with initial velocity v comes with a distance a_q of a $\bar{q}$, its velocity changes by

$$\frac{\Delta v}{v} \sim \frac{1}{v}\frac{F}{m_X}\Delta t \sim \frac{1}{v}\frac{F}{m_X}\frac{a_q}{v} \sim \frac{\alpha_D^2 m_q}{m_X v^2} \sim 1\,.$$

- The change in the position of X due to the force is

$$\frac{\Delta r}{a_q} \sim \frac{1}{a_q}\frac{F\Delta t^2}{m_X} \sim \frac{\alpha_D^2 m_q}{m_X v^2} \sim 1\,.$$

Rearrangement Hamiltonian

The full interacting Hamiltonian includes terms that couple all heavy and light dof:

$$\begin{aligned}
\mathcal{H}_{\text{free}} &= -\frac{1}{m_X}\nabla_R^2 - \frac{1}{2m_q}\nabla_{r_q}^2 - \frac{1}{2m_q}\nabla_{r_{\bar{q}}}^2 \,, \\
\mathcal{H}_{\text{int}} &= V_{X\bar{X}}\left(R\right) + V_{q\bar{q}}\left(|\boldsymbol{r}_q - \boldsymbol{r}_{\bar{q}}|\right) + \mathcal{H}_{\text{tr}} \,, \\
\mathcal{H}_{\text{tr}} &= V_{q\bar{X}}\left(|\boldsymbol{r}_q + \boldsymbol{R}/2|\right) + V_{\bar{q}X}\left(|\boldsymbol{r}_{\bar{q}} - \boldsymbol{R}/2|\right) \\
&\quad - V_{\bar{q}\bar{X}}\left(|\boldsymbol{r}_{\bar{q}} + \boldsymbol{R}/2|\right) - V_{qX}\left(|\boldsymbol{r}_q - \boldsymbol{R}/2|\right)
\end{aligned}$$

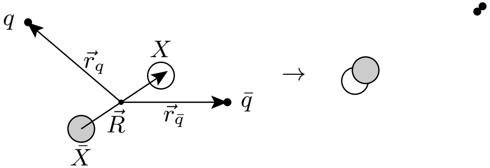

Rearrangement Hamiltonian

The full interacting Hamiltonian includes terms that couple all heavy and light dof:

$$
\begin{aligned}
\mathcal{H}_{\text{free}} &= -\frac{1}{m_X}\nabla_R^2 - \frac{1}{2m_q}\nabla_{r_q}^2 - \frac{1}{2m_q}\nabla_{r_{\bar{q}}}^2 \,, \\
\mathcal{H}_{\text{int}} &= V_{X\bar{X}}\left(R\right) + V_{q\bar{q}}\left(|\boldsymbol{r}_q - \boldsymbol{r}_{\bar{q}}|\right) + \mathcal{H}_{\text{tr}} \,, \\
\mathcal{H}_{\text{tr}} &= V_{q\bar{X}}\left(|\boldsymbol{r}_q + \boldsymbol{R}/2|\right) + V_{\bar{q}X}\left(|\boldsymbol{r}_{\bar{q}} - \boldsymbol{R}/2|\right) \\
&\quad - V_{\bar{q}\bar{X}}\left(|\boldsymbol{r}_{\bar{q}} + \boldsymbol{R}/2|\right) - V_{qX}\left(|\boldsymbol{r}_q - \boldsymbol{R}/2|\right)
\end{aligned}
$$

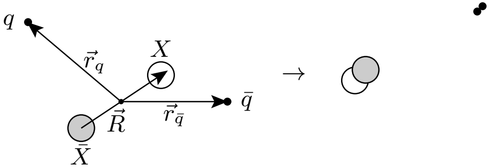

NB: we have taken the states to be in the Coulombic regime, so $V(r) \propto \pm \frac{\bar{\alpha}_D}{r}$.

Multichannel Scattering

$$H_X + \bar{H}_X \to \left(X\bar{X}\right) + (q\bar{q})$$

- Final: eigenstate of free Hamiltonian and $V_{X\bar{X}} + V_{q\bar{q}}$.
- Initial: eigenstate of free Hamiltonian plus $V_{q\bar{X}} + V_{\bar{q}X}$.

Multichannel Scattering

$$H_X + \bar{H}_X \to \left(X\bar{X}\right) + (q\bar{q})$$

- Final: eigenstate of free Hamiltonian and $V_{X\bar{X}} + V_{q\bar{q}}$.
- Initial: eigenstate of free Hamiltonian plus $V_{q\bar{X}} + V_{\bar{q}X}$.
- The asymptotic states lie in different channels, and $\mathcal{H}_{\rm tr}$ mediates the interaction.

Multichannel Scattering

$$H_X + \bar{H}_X \to \left(X\bar{X}\right) + (q\bar{q})$$

- Final: eigenstate of free Hamiltonian and $V_{X\bar{X}} + V_{q\bar{q}}$.
- Initial: eigenstate of free Hamiltonian plus $V_{q\bar{X}} + V_{\bar{q}X}$.
- The asymptotic states lie in different channels, and $\mathcal{H}_{\mathrm{tr}}$ mediates the interaction.
- Want to separate the total wavefunction for the initial and final states into products of wavefunctions for light and heavy dof:

$$\Psi = \psi^{q\bar{q}}\left(\mathbf{R}, \mathbf{r}_q, \mathbf{r}_{\bar{q}}\right) \cdot \psi^{X\bar{X}}\left(\mathbf{R}\right).$$

Multichannel Scattering

$$H_X + \bar{H}_X \to \left(X\bar{X}\right) + (q\bar{q})$$

- Final: eigenstate of free Hamiltonian and $V_{X\bar{X}} + V_{q\bar{q}}$.
- Initial: eigenstate of free Hamiltonian plus $V_{q\bar{X}} + V_{\bar{q}X}$.
- The asymptotic states lie in different channels, and $\mathcal{H}_{\rm tr}$ mediates the interaction.
- Want to separate the total wavefunction for the initial and final states into products of wavefunctions for light and heavy dof:

$$\Psi = \psi^{q\bar{q}}\left(\mathbf{R}, \mathbf{r}_q, \mathbf{r}_{\bar{q}}\right) \cdot \psi^{X\bar{X}}\left(\mathbf{R}\right).$$

- Easy to see for final state: $\psi_f^{X\bar{X}}$ and $\psi_f^{q\bar{q}}$ are standard bound state solutions (for Coulomb potential), multiplied by a plane wave for the translational motion of the $q\bar{q}$.

Initial-State Wavefunction: Born-Oppenheimer Approximation

- Asymptotically at large R for initial states, residual interaction terms in the Hamiltonian produce a van der Waals-like force since the $q, \bar{q}$ are bound in $H_X, \bar{H}_X$.

Initial-State Wavefunction: Born-Oppenheimer Approximation

- Asymptotically at large R for initial states, residual interaction terms in the Hamiltonian produce a van der Waals-like force since the $q, \bar{q}$ are bound in $H_X, \bar{H}_X$.
- Use the Born-Oppenheimer approximation to separate dynamics of light and heavy dof in the initial state.

Initial-State Wavefunction: Born-Oppenheimer Approximation

- Asymptotically at large R for initial states, residual interaction terms in the Hamiltonian produce a van der Waals-like force since the $q, \bar{q}$ are bound in $H_X, \bar{H}_X$.
- Use the Born-Oppenheimer approximation to separate dynamics of light and heavy dof in the initial state.
- First, we solve for light dof with fixed positions for the heavy dof:

$$\left(-\frac{1}{2m_q}\nabla^2_{r_q} - \frac{1}{2m_q}\nabla^2_{r_{\bar{q}}} + V_{q\bar{q}} + \mathcal{H}_{\text{tr}}\right)\psi_i^{q\bar{q}} = V_{\text{BO}}(\mathbf{R})\psi_i^{q\bar{q}}\,.$$

Initial-State Wavefunction: Born-Oppenheimer Approximation

- Asymptotically at large R for initial states, residual interaction terms in the Hamiltonian produce a van der Waals-like force since the $q, \bar{q}$ are bound in $H_X, \bar{H}_X$.
- Use the Born-Oppenheimer approximation to separate dynamics of light and heavy dof in the initial state.
- First, we solve for light dof with fixed positions for the heavy dof:

$$\left(-\frac{1}{2m_q}\nabla^2_{r_q} - \frac{1}{2m_q}\nabla^2_{r_{\bar{q}}} + V_{q\bar{q}} + \mathcal{H}_{\mathrm{tr}}\right)\psi_i^{q\bar{q}} = V_{\mathrm{BO}}(\mathbf{R})\psi_i^{q\bar{q}}\,.$$

- Solve for the heavy dof with distorted potential from light dof:

$$\left(-\frac{1}{m_X}\nabla^2_R + V_{X\bar{X}}(R) + V_{\mathrm{BO}}(\mathbf{R})\right)\psi_i^{X\bar{X}} = E_i\psi_i^{X\bar{X}}\,.$$

Initial-State Wavefunction: Born-Oppenheimer Approximation

- Asymptotically at large R for initial states, residual interaction terms in the Hamiltonian produce a van der Waals-like force since the $q, \bar{q}$ are bound in $H_X, \bar{H}_X$.
- Use the Born-Oppenheimer approximation to separate dynamics of light and heavy dof in the initial state.
- First, we solve for light dof with fixed positions for the heavy dof:

$$\left(-\frac{1}{2m_q}\nabla^2_{r_q} - \frac{1}{2m_q}\nabla^2_{r_{\bar{q}}} + V_{q\bar{q}} + \mathcal{H}_{\mathrm{tr}}\right)\psi_i^{q\bar{q}} = V_{\mathrm{BO}}(\mathbf{R})\psi_i^{q\bar{q}}\,.$$

- Solve for the heavy dof with distorted potential from light dof:

$$\left(-\frac{1}{m_X}\nabla^2_R + V_{X\bar{X}}(R) + V_{\mathrm{BO}}(\mathbf{R})\right)\psi_i^{X\bar{X}} = E_i\psi_i^{X\bar{X}}\,.$$

- $V_{\mathrm{BO}}(\mathbf{R})$ should interpolate between
  - at large R (initial state): twice the binding energy of H_X, $\bar{\alpha}_D^2 m_q$,
  - at small R (final state): the q-onium binding energy, $-\bar{\alpha}_D^2 m_q/4$.

Potentials

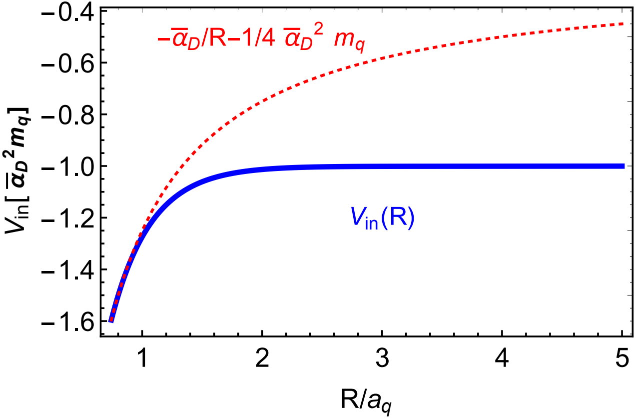

- Effective potential for X–$\bar{X}$: $V_{\rm in} = V_{X\bar{X}} + V_{\rm BO}$.
- BO potentials taken from results of studies of H–$\bar{\mathrm{H}}$ rearrangement. Strasburger, J. Phys. B 35 L435 (2002)
- Asymptotics determine phase matching of $\psi_i^{X\bar{X}}$ at the screening distance:

$$\sum_l i^l \sqrt{(2l+1)}\, e^{i\delta_l}\, [\cos\delta_l\, j_l(kR) - \sin\delta_l\, n_l(kR)]\, Y_{l0}(\theta_R)\,.$$

Wavefunctions

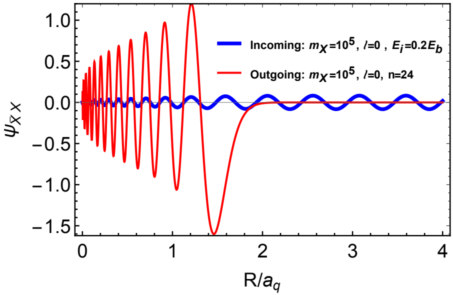

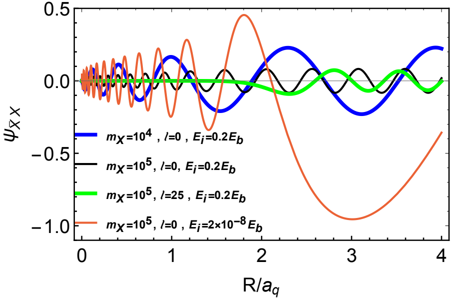

Shut Up and Calculate?

- In position space, the matrix element and transition amplitude are

$$\mathcal{M} = \int d^3\mathbf{R} \;\; \psi_f^{X\bar{X}*}\left(\mathbf{R}\right) \psi_i^{X\bar{X}}\left(\mathbf{R}\right) T\left(\mathbf{R}\right) \, ,$$

$$T\left(\mathbf{R}\right) = \int d^3\mathbf{r}_q \; d^3\mathbf{r}_{\bar{q}} \;\; \psi_f^{q\bar{q}*}\left(\mathbf{r}_q, \mathbf{r}_{\bar{q}}\right) \mathcal{H}_{\mathrm{tr}} \, \psi_i^{q\bar{q}}\left(\mathbf{R}; \mathbf{r}_q, \mathbf{r}_{\bar{q}}\right) \, .$$

Shut Up and Calculate?

- In position space, the matrix element and transition amplitude are

$$\mathcal{M} = \int d^3\mathbf{R}\ \psi_f^{X\bar{X}*}(\mathbf{R})\ \psi_i^{X\bar{X}}(\mathbf{R})\ T(\mathbf{R})\ ,$$
$$T(\mathbf{R}) = \int d^3\mathbf{r}_q\ d^3\mathbf{r}_{\bar{q}}\ \psi_f^{q\bar{q}*}(\mathbf{r}_q, \mathbf{r}_{\bar{q}})\ \mathcal{H}_{\mathrm{tr}}\, \psi_i^{q\bar{q}}(\mathbf{R}; \mathbf{r}_q, \mathbf{r}_{\bar{q}})\ .$$

- Calculating with full $T(\mathbf{R})$ is complicated. Assume spherical symmetry.

Shut Up and Calculate?

- In position space, the matrix element and transition amplitude are

$$\mathcal{M} = \int d^3\mathbf{R}\ \psi_f^{X\bar{X}*}(\mathbf{R})\ \psi_i^{X\bar{X}}(\mathbf{R})\ T(\mathbf{R})\ ,$$

$$T(\mathbf{R}) = \int d^3\mathbf{r}_q\ d^3\mathbf{r}_{\bar{q}}\ \psi_f^{q\bar{q}*}(\mathbf{r}_q, \mathbf{r}_{\bar{q}})\ \mathcal{H}_{\mathrm{tr}}\, \psi_i^{q\bar{q}}(\mathbf{R}; \mathbf{r}_q, \mathbf{r}_{\bar{q}})\ .$$

- Calculating with full $T(\mathbf{R})$ is complicated. Assume spherical symmetry.
- The Born-Oppenheimer approximation is independent of the mass m_X, so we can use the results from H–$\bar{\mathrm{H}}$ rearrangement. Jonsell et al., PRA 64 (2001) 052712

$$T(R) = \begin{cases} \beta_T E_f & R \lesssim 3/4\, a_q \\ 0 & R \gtrsim 3/4\, a_q \end{cases} .$$

Shut Up and Calculate?

- In position space, the matrix element and transition amplitude are

$$\mathcal{M} = \int d^3\mathbf{R}\ \psi_f^{X\bar{X}*}(\mathbf{R})\ \psi_i^{X\bar{X}}(\mathbf{R})\ T(\mathbf{R})\ ,$$

$$T(\mathbf{R}) = \int d^3\mathbf{r}_q\ d^3\mathbf{r}_{\bar{q}}\ \psi_f^{q\bar{q}*}(\mathbf{r}_q, \mathbf{r}_{\bar{q}})\ \mathcal{H}_{\mathrm{tr}}\,\psi_i^{q\bar{q}}(\mathbf{R}; \mathbf{r}_q, \mathbf{r}_{\bar{q}})\ .$$

- Calculating with full $T(\mathbf{R})$ is complicated. Assume spherical symmetry.
- The Born-Oppenheimer approximation is independent of the mass m_X, so we can use the results from H–$\bar{\mathrm{H}}$ rearrangement. Jonsell et al., PRA 64 (2001) 052712

$$T(R) = \begin{cases} \beta_T E_f & R \lesssim 3/4\, a_q \\ 0 & R \gtrsim 3/4\, a_q \end{cases}\ .$$

- Actually, only the result near $R \approx a_q$ is needed.
- The dependence on the bound state spectrum is encapsulated in E_f, the kinetic energy of the final state.

Results for Partial Waves

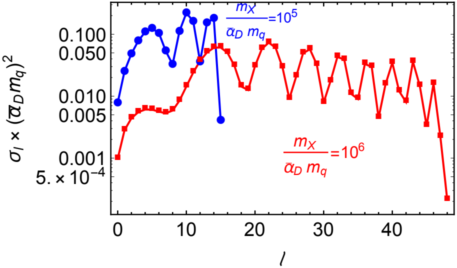

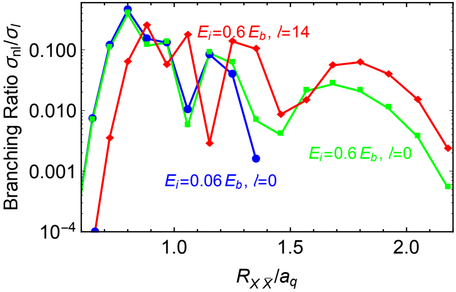

Results for Partial Waves

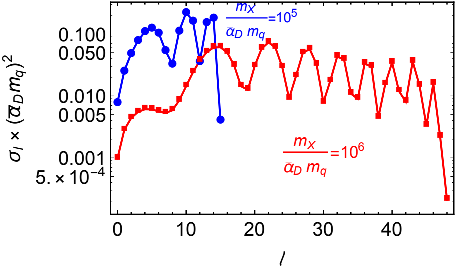

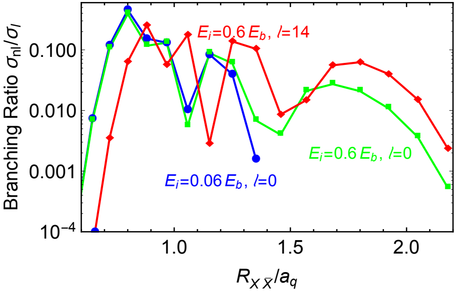

- Left: $\bar{\alpha}_D \approx 1/137$, cross section shuts off at classical $l_{\max}$.
- Right: cross section dominated by formation of quarkonia states with size $\approx a_q$.

Results

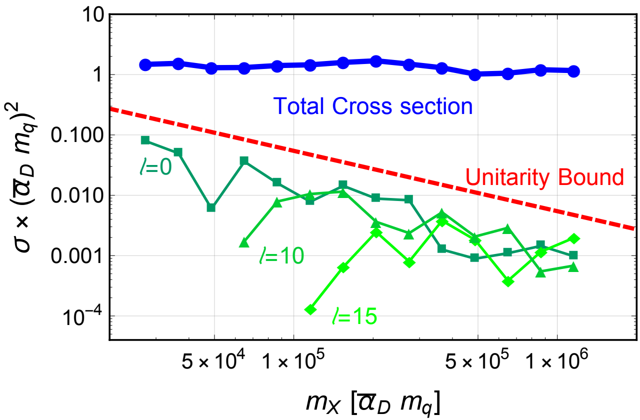
10
1
0.100
0.010
0.001
10^{-4}
$\sigma \times (\overline{\alpha}_D\ m_q)^2$
Total Cross section
Unitarity Bound
l=0
l=10
l=15
5×10^4
1×10^5
5×10^5
1×10^6
$m_X\ [\overline{\alpha}_D\ m_q]$

Results

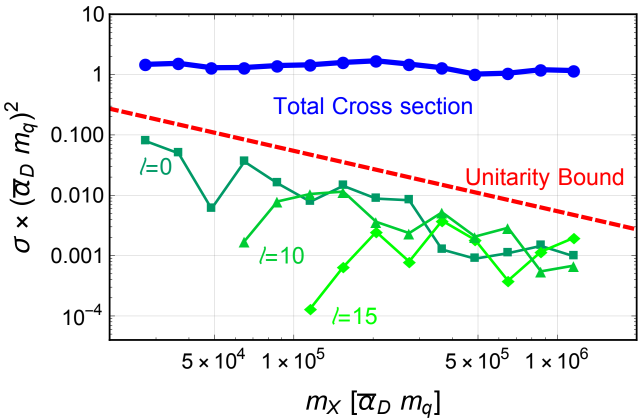

- blue: total $\sigma_{\rm rearr}$ for $E_i = (0.6)\bar{\alpha}_D^2 m_q$ is indeed geometric.
- red: unitarity bound $4\pi/k_i^2$.
- greens: partial waves normalized by $2l+1$.

Summary

- Take-away: many partial waves are important in rearrangement process.

Summary

- Take-away: many partial waves are important in rearrangement process.
- Each partial wave saturates the unitarity bound with

$$\sigma_l \sim \frac{1}{k_i^2}(2l+1)\,.$$

Summary

- Take-away: many partial waves are important in rearrangement process.
- Each partial wave saturates the unitarity bound with

$$\sigma_l \sim \frac{1}{k_i^2}(2l+1)\,.$$

- Summing all partial waves,

$$\sigma \sim \frac{l_{\mathrm{max}}^2}{k_i^2}\,.$$

Summary

- Take-away: many partial waves are important in rearrangement process.
- Each partial wave saturates the unitarity bound with

$$\sigma_l \sim \frac{1}{k_i^2}(2l+1)\,.$$

- Summing all partial waves,

$$\sigma \sim \frac{l_{\max}^2}{k_i^2}\,.$$

- Since the maximum angular momentum is roughly given by the classical angular momentum $l_{\max} = k_i a_q$, we have

$$\sigma \sim a_q^2\,,$$

which depends only on the scale of the light dof.

Outline

BSF by Emission of Light Bosons

- There are extensive examples in the literature of bound-state formation via emission of light bosons, e.g., dark photons or (pseudo)-scalars.
- Together with Sommerfeld enhancement from long-range forces, can produce nontrivial effect in halos and structure formation.
  - Dissipation affects the size and morphology of halos.
  - Compton scattering off hidden photons delays kinetic decoupling, modifying small-scale structure.
  - Enhance DM annihilation in halos.

Feng, Kaplinghat, Tu, Yu 0905.3039; Petraki, Pearce, Kusenko 1403.1077; Agrawal, Cyr-Racine, Randall, Scholtz 1610.04611

- It is known that bound states that use a $U(1)$ force have a small effect on present relic density.
- Is this still true if the bound state is governed by a confining force, but formed through perturbative emission of a vector?

Schematically

$$\underbrace{H_X + \bar{H}_X}_{\mathcal{U}} \to \underbrace{(X\bar{X})}_{\mathcal{B}} + \gamma, \varphi$$

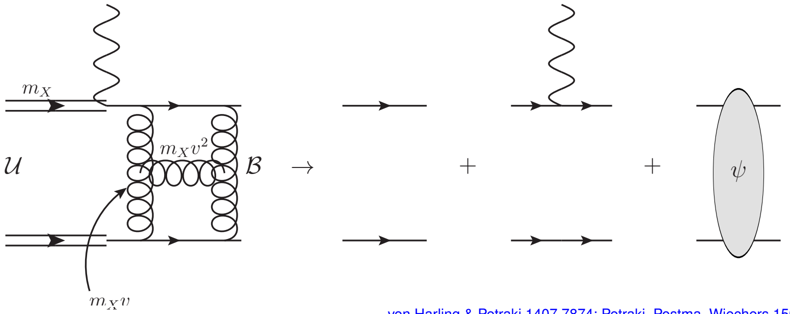

von Harling & Petraki 1407.7874; Petraki, Postma, Wiechers 1505.00109

Petraki, Postma, de Vries 1611.01394; Cirelli et al. 1612.07295

Solving for the Wavefunctions

Dimensionless Schrödinger equation and effective potential:

$$-\chi''_{nl}(x) + V_{\text{eff}}(x)\chi_{nl}(x) = \epsilon_{nl}\chi_{nl}(x)\,,$$

$$V_{\text{eff}}(x) = \frac{l(l+1)}{x^2} + \Theta(x - x_c)\left(-a_D\left(\frac{1}{x} - \frac{1}{x_c}\right) + x - x_c\right)\,,$$

Solving for the Wavefunctions

Dimensionless Schrödinger equation and effective potential:

$$-\chi''_{nl}(x) + V_{\rm eff}(x)\chi_{nl}(x) = \epsilon_{nl}\chi_{nl}(x)\,,$$
$$V_{\rm eff}(x) = \frac{l(l+1)}{x^2} + \Theta(x-x_c)\left(-a_D\left(\frac{1}{x}-\frac{1}{x_c}\right)+x-x_c\right)\,,$$

with scalings $\epsilon = E/E_0, x = r/r_0$:

$$r_0 = \frac{1}{\Lambda_D}\left(\frac{\Lambda_D}{m_X}\right)^{1/3}\,,\quad E_0 = \Lambda_D\left(\frac{\Lambda_D}{m_X}\right)^{1/3}\,.$$

Solving for the Wavefunctions

Dimensionless Schrödinger equation and effective potential:

$$-\chi''_{nl}(x) + V_{\text{eff}}(x)\chi_{nl}(x) = \epsilon_{nl}\chi_{nl}(x)\,,$$

$$V_{\text{eff}}(x) = \frac{l(l+1)}{x^2} + \Theta(x - x_c)\left(-a_D\left(\frac{1}{x} - \frac{1}{x_c}\right) + x - x_c\right)\,,$$

with scalings $\epsilon = E/E_0, x = r/r_0$:

$$r_0 = \frac{1}{\Lambda_D}\left(\frac{\Lambda_D}{m_X}\right)^{1/3}\,, \quad E_0 = \Lambda_D\left(\frac{\Lambda_D}{m_X}\right)^{1/3}\,.$$

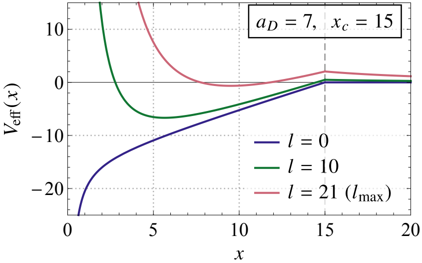

- Effective potential has minimum at

$$x_{\text{min}} = (2l(l+1))^{1/3}\,.$$

- Then l_{max} for bound states is governed by condition that

$$x_{\text{min}}(l_{\text{max}}) \leq x_c\,.$$

Wavefunctions

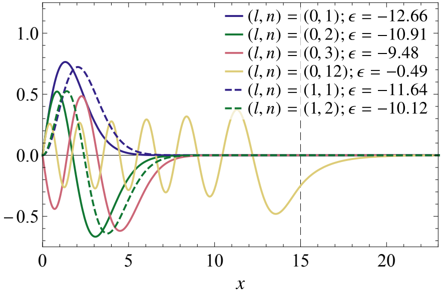

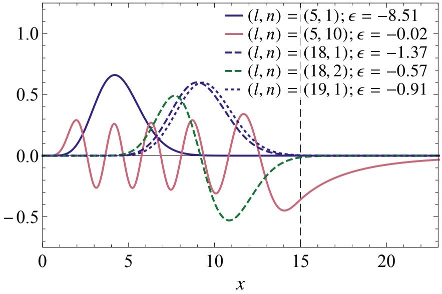

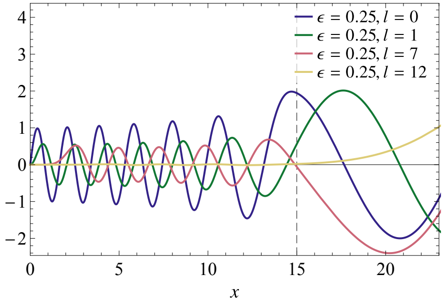

Near-threshold states (both bound and scattering) have largest overlap.

Computing the Cross Section

- Employ standard methods in QFT for computing 2–2 cross section.

Computing the Cross Section

- Employ standard methods in QFT for computing 2–2 cross section.
- In nonrelativistic approximation, the matrix element reduces to an overlap integral between scattering and bound-state wavefunctions.

Computing the Cross Section

- Employ standard methods in QFT for computing 2–2 cross section.
- In nonrelativistic approximation, the matrix element reduces to an overlap integral between scattering and bound-state wavefunctions.
- The dipole approximation for the emitted radiation leads to a selection rule relating the angular momenta of initial final states.

Computing the Cross Section

- Employ standard methods in QFT for computing 2–2 cross section.
- In nonrelativistic approximation, the matrix element reduces to an overlap integral between scattering and bound-state wavefunctions.
- The dipole approximation for the emitted radiation leads to a selection rule relating the angular momenta of initial final states.
- The result is

$$v_{\rm rel}\,\sigma_{k\hat{\mathbf{z}}\to nl} = \frac{2e_X^2}{m_X^2}\left(\frac{\Lambda_D}{m_X}\right)^{2/3}(\epsilon_k-\epsilon_{nl})^3\left[(l+1)\left|I_{k,l+1\to nl}\right|^2 + l\left|I_{k,l-1\to nl}\right|^2\right],$$

Computing the Cross Section

- Employ standard methods in QFT for computing 2–2 cross section.
- In nonrelativistic approximation, the matrix element reduces to an overlap integral between scattering and bound-state wavefunctions.
- The dipole approximation for the emitted radiation leads to a selection rule relating the angular momenta of initial final states.
- The result is

$$v_{\mathrm{rel}}\,\sigma_{k\hat{\mathbf{z}}\to nl} = \frac{2e_X^2}{m_X^2}\left(\frac{\Lambda_D}{m_X}\right)^{2/3}(\epsilon_k-\epsilon_{nl})^3\left[(l+1)\left|I_{k,l+1\to nl}\right|^2 + l\left|I_{k,l-1\to nl}\right|^2\right],$$

where $\epsilon_k = \frac{E_k}{E_0}$ and I is the radial wavefunction overlap integral

$$I_{k,l\pm1\to nl} = \int dx\, x\, \chi^*_{nl}(x)\chi_{k,l\pm1}(x)\,.$$

Computing the Cross Section

- Employ standard methods in QFT for computing 2–2 cross section.
- In nonrelativistic approximation, the matrix element reduces to an overlap integral between scattering and bound-state wavefunctions.
- The dipole approximation for the emitted radiation leads to a selection rule relating the angular momenta of initial final states.
- The result is

$$v_{\rm rel}\,\sigma_{k\hat{\mathbf{z}}\to nl} = \frac{2e_X^2}{m_X^2}\left(\frac{\Lambda_D}{m_X}\right)^{2/3}(\epsilon_k-\epsilon_{nl})^3\left[(l+1)\left|I_{k,l+1\to nl}\right|^2 + l\left|I_{k,l-1\to nl}\right|^2\right],$$

where $\epsilon_k = \frac{E_k}{E_0}$ and I is the radial wavefunction overlap integral

$$I_{k,l\pm1\to nl} = \int dx\, x\,\chi_{nl}^*(x)\chi_{k,l\pm1}(x)\,.$$

- Thermal averaging with Maxwell-Boltzmann distribution:

$$f_{\rm MB}(\boldsymbol{p}) = \left(\frac{2\pi\beta}{m}\right)^{3/2}\exp\left(-\frac{\beta|\boldsymbol{p}|^2}{2m_X}\right),$$

$$\langle v_{\rm rel}\sigma_{\rm BSF}\rangle = \sqrt{\frac{16\beta^3}{\pi m_X^3}}\int dk\, k^2\, e^{-\beta k^2/m_X}\,(v_{\rm rel}\sigma_{\rm BSF})_k\,,$$

Radiative BSF: Overlap Integral

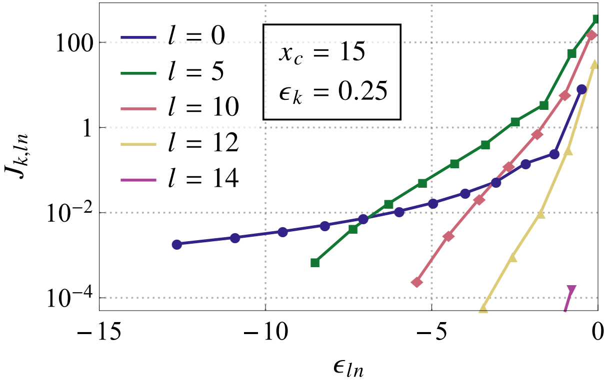

Shallowest bound states give the largest contribution to overlap.

Results

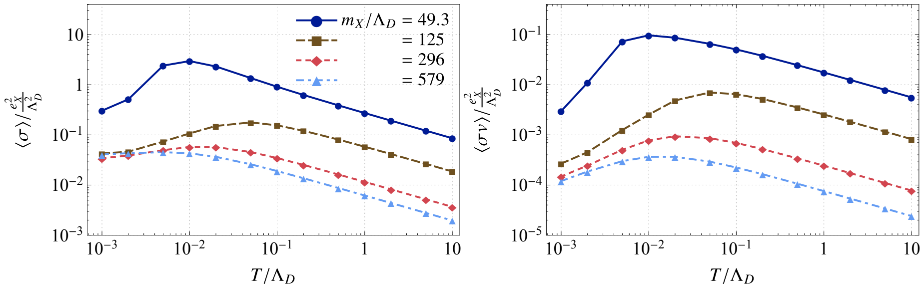

$m_X/\Lambda_D = 49.3$
$= 125$
$= 296$
$= 579$
$\langle\sigma\rangle / \frac{e_X^2}{\Lambda_D^2}$
$\langle\sigma v\rangle / \frac{e_X^2}{\Lambda_D^2}$
T/Λ_D
T/Λ_D

Results

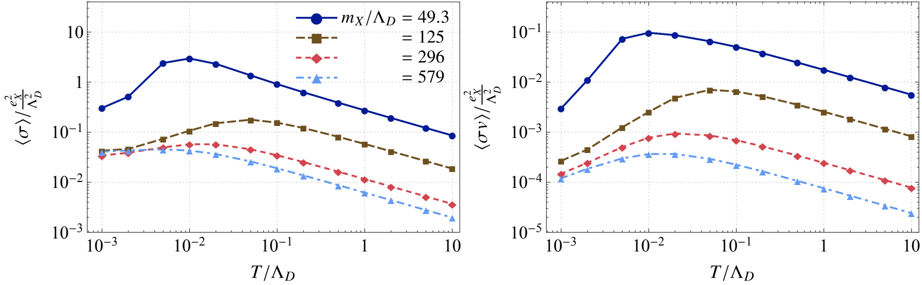

For large hierarchies, the cross section is not geometric.

Results

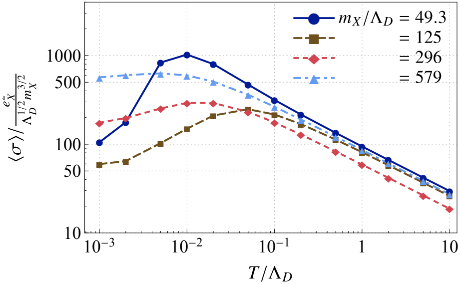

$m_X/\Lambda_D = 49.3$
$= 125$
$= 296$
$= 579$
$\langle\sigma\rangle / \frac{e_X^2}{\Lambda_D^{1/2} m_X^{3/2}}$
T/Λ_D

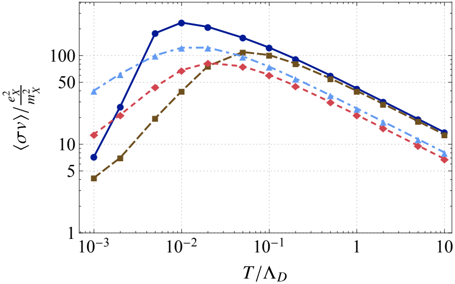

$\langle\sigma v\rangle / \frac{e_X^2}{m_X^2}$
T/Λ_D

Results

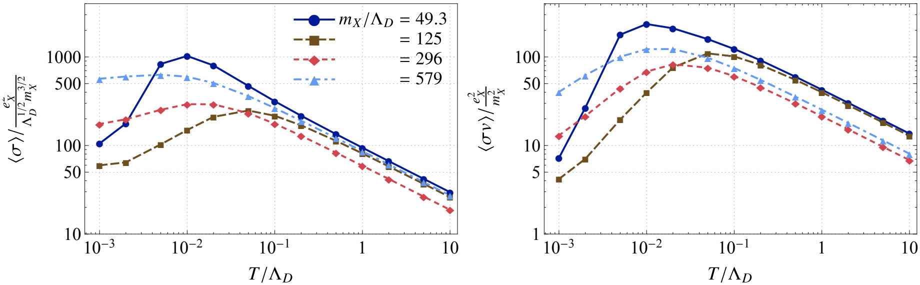

Agrees with semiclassical expectation from Larmor: $m_X^{-3/2}$ scaling.

Summary

- For larger mass hierarchies, the cross section is not geometric.

Summary

- For larger mass hierarchies, the cross section is not geometric.
- The cross section approaches an asymptotic value for lower temperatures.
- Then $\langle \sigma v \rangle$ will decrease at lower temperatures, so this process will never dominate.

Summary

- For larger mass hierarchies, the cross section is not geometric.
- The cross section approaches an asymptotic value for lower temperatures.
- Then $\langle \sigma v \rangle$ will decrease at lower temperatures, so this process will never dominate.
- Our calculation was largely independent of spin of light state, so should hold for emission of scalars as well.
- Major difference with rearrangement: light dof are spectators in the perturbative process, only entered parametrically through the final-state wavefunctions.

Outline

Cosmology

- Second stage should be over fairly quickly, as depletion is faster nearer to confinement temperature (larger number density).

Cosmology

- Second stage should be over fairly quickly, as depletion is faster nearer to confinement temperature (larger number density).
- Standard freeze-out relic density parameter:

$$\Omega_X^{\mathrm{ann}} h^2 \sim \frac{10^{-9}\,\mathrm{GeV}^{-2}}{\langle \sigma_X^{\mathrm{ann}} v \rangle} \sim \left(\frac{m_X}{10\,\mathrm{TeV}} \right)^2 \frac{1}{\alpha_D^2(m_X)} \,.$$

Cosmology

- Second stage should be over fairly quickly, as depletion is faster nearer to confinement temperature (larger number density).
- Standard freeze-out relic density parameter:

$$\Omega_X^{\rm ann} h^2 \sim \frac{10^{-9}\,{\rm GeV}^{-2}}{\langle \sigma_X^{\rm ann} v \rangle} \sim \left(\frac{m_X}{10\,{\rm TeV}} \right)^2 \frac{1}{\alpha_D^2(m_X)} \,.$$

- After second stage of annihilation:

$$\frac{\Omega_{H_X}}{\Omega_X^{\rm ann}} \sim \sqrt{\frac{\Lambda_D}{m_X}} \,.$$

Cosmology

- Second stage should be over fairly quickly, as depletion is faster nearer to confinement temperature (larger number density).
- Standard freeze-out relic density parameter:

$$\Omega_X^{\mathrm{ann}} h^2 \sim \frac{10^{-9}\,\mathrm{GeV}^{-2}}{\langle \sigma_X^{\mathrm{ann}} v \rangle} \sim \left(\frac{m_X}{10\,\mathrm{TeV}} \right)^2 \frac{1}{\alpha_D^2(m_X)} .$$

- After second stage of annihilation:

$$\frac{\Omega_{H_X}}{\Omega_X^{\mathrm{ann}}} \sim \sqrt{\frac{\Lambda_D}{m_X}} .$$

- With large hierarchy, can dilute the relic density of $H_X, \bar{H}_X$.

Multicomponent DM

- Other hadronic states in the spectrum with multiple X's, but some amount of light q's are likely to have second-state annihilations with geometric cross sections.

Multicomponent DM

- Other hadronic states in the spectrum with multiple X's, but some amount of light q's are likely to have second-state annihilations with geometric cross sections.
- Chain of processes for $N > 2$: H_X–H_X scattering can also double X baryons, which can continue to interact with other H_X's in the plasma to form triple X baryons, etc.
- Since these interactions all involve the brown muck, we expect them to have geometric cross sections.

Multicomponent DM

- Other hadronic states in the spectrum with multiple X's, but some amount of light q's are likely to have second-state annihilations with geometric cross sections.
- Chain of processes for $N > 2$: H_X–H_X scattering can also double X baryons, which can continue to interact with other H_X's in the plasma to form triple X baryons, etc.
- Since these interactions all involve the brown muck, we expect them to have geometric cross sections.
- The X's inside these baryons are also stable, so we can have a multitude of DM states.
- Future work: solve Boltzmann equation with these dynamics to find equilibrium yields.

Phenomenology

- Collider pheno: studies on dark jets at the LHC. Schwaller, Stolarski, Weiler 1502.05409; Cohen, Lisanti, Lou 1503.00009 + Mishra-Sharma 1707.05326; Park, Zhang 1712.09279

Phenomenology

- Collider pheno: studies on dark jets at the LHC. Schwaller, Stolarski, Weiler 1502.05409; Cohen, Lisanti, Lou 1503.00009 + Mishra-Sharma 1707.05326; Park, Zhang 1712.09279
- Direct detection: couplings to SM are described by effective operators, other energy ranges for DD opened by multitude of final states.

Phenomenology

- Collider pheno: studies on dark jets at the LHC. Schwaller, Stolarski, Weiler 1502.05409; Cohen, Lisanti, Lou 1503.00009 + Mishra-Sharma 1707.05326; Park, Zhang 1712.09279
- Direct detection: couplings to SM are described by effective operators, other energy ranges for DD opened by multitude of final states.
- Indirect detection:
  - Heavy DM can access many hadronic states below confining temperature, could give a boost to signals from dwarf galaxies.
  - Self-interaction with large cross sections can yield interesting halo dynamics (and are constrained by such).

Conclusion

- Nonabelian, confining hidden sectors with both heavy and light states are natural frameworks for rich dark matter sectors that include bound states.

Conclusion

- Nonabelian, confining hidden sectors with both heavy and light states are natural frameworks for rich dark matter sectors that include bound states.
- Below the confinement temperature, these bound states can have nonstandard cosmology by undergoing an additional annihilation phase.
- A large geometric cross section for bound state formation in the second stage is required in order that the present relic density deviate from the result from standard (s-wave annihilation) freeze-out.

Conclusion

- Nonabelian, confining hidden sectors with both heavy and light states are natural frameworks for rich dark matter sectors that include bound states.
- Below the confinement temperature, these bound states can have nonstandard cosmology by undergoing an additional annihilation phase.
- A large geometric cross section for bound state formation in the second stage is required in order that the present relic density deviate from the result from standard (s-wave annihilation) freeze-out.
- The above is achieved in the rearrangement process, which accesses all partial waves, but not in the process of BSF via radiative emission.

Conclusion

- Nonabelian, confining hidden sectors with both heavy and light states are natural frameworks for rich dark matter sectors that include bound states.
- Below the confinement temperature, these bound states can have nonstandard cosmology by undergoing an additional annihilation phase.
- A large geometric cross section for bound state formation in the second stage is required in order that the present relic density deviate from the result from standard (s-wave annihilation) freeze-out.
- The above is achieved in the rearrangement process, which accesses all partial waves, but not in the process of BSF via radiative emission.
- There are manifold possibilities for exploring further consequences in DM cosmology and phenomenology.

Conclusion

- Nonabelian, confining hidden sectors with both heavy and light states are natural frameworks for rich dark matter sectors that include bound states.
- Below the confinement temperature, these bound states can have nonstandard cosmology by undergoing an additional annihilation phase.
- A large geometric cross section for bound state formation in the second stage is required in order that the present relic density deviate from the result from standard (s-wave annihilation) freeze-out.
- The above is achieved in the rearrangement process, which accesses all partial waves, but not in the process of BSF via radiative emission.
- There are manifold possibilities for exploring further consequences in DM cosmology and phenomenology.

Thank you.

Partial Waves

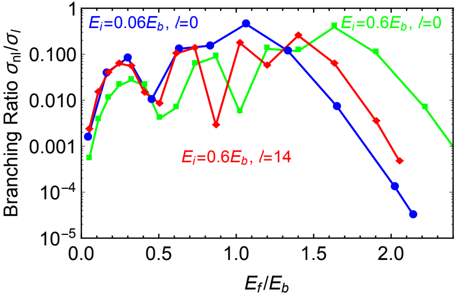

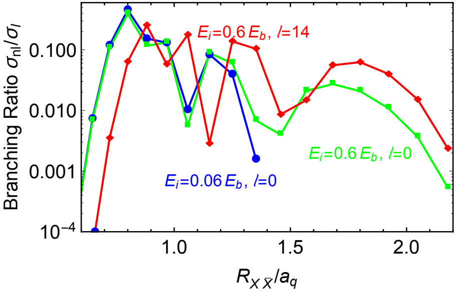

Results from H–$\bar{\mathrm{H}}$

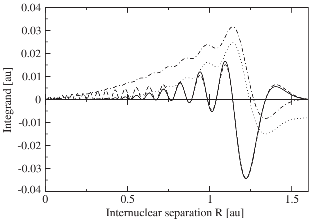

Figure 1. The integrand in equation (6) calculated using the full R dependence of the leptonic matrix element (solid line), and using the approximation that the overlap between initial and final is constant leptonic wavefunctions (see equation (9)) (dashed line). We also show their integrals from 0 to R (multiplied by 10) as the dotted line and the dash–dotted line, respectively. The dash–dotted line shows that the constant overlap approximation yields a vanishing T matrix, while the dotted line shows that the small change in the integrand induced by including the R dependence of the overlap results in a non-vanishing T matrix.

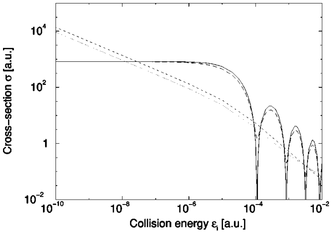

FIG. 6. Cross sections for the H-$\bar{\mathrm{H}}$ system: elastic cross section obtained from the real part of the phase shift only (solid), elastic cross section including correction for the presence of inelastic scattering (long dashed), rearrangement cross section (dotted), and proton-antiproton annihilation in flight (dashed). At low energies, the elastic cross section is 823 without the correction for inelastic scattering, and 829 including this correction, while the low-energy behavior of σ^{rearr} is $0.09/\sqrt{\epsilon_i}$, and $\sigma_a^{p\bar{p}} \sim 0.14/\sqrt{\epsilon_i}$.

Rearrangement at Low Temperatures: H–$\bar{\mathrm{H}}$

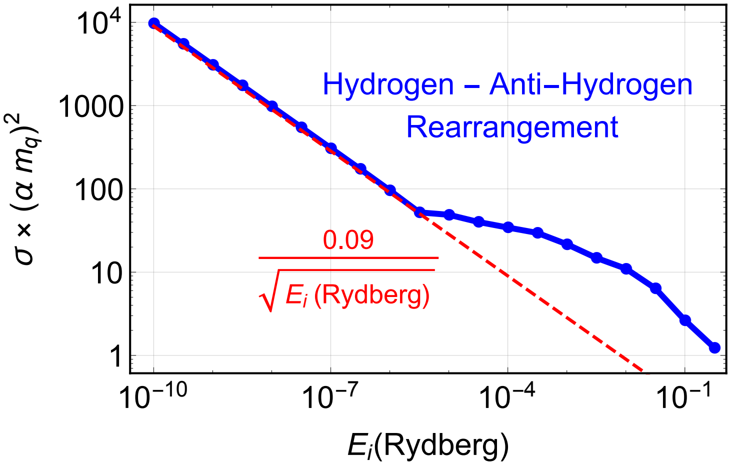

More Wavefunctions in Radiative BSF

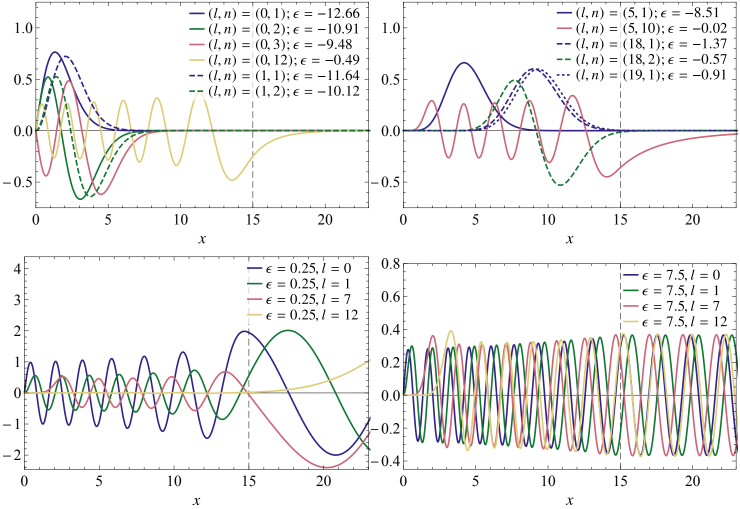

- Bound states with "radial number" n have $n-1$ nodes.
- Shallower bound states with smaller l tend to penetrate into the region beyond $x > x_c$.
- Scattering states with larger ϵ and smaller l have larger penetration to $x < x_c$.